Journal of Biomechanics 44 (2011) 2129–2135

Contents lists available at ScienceDirect

Journal of Biomechanics

journal homepage: www.elsevier.com/locate/jbiomech
www.JBiomech.com

In-vivo determination of 3D muscle architecture of human muscle using free hand ultrasound

Manku Rana *, James M. Wakeling

Department of Biomedical Physiology and Kinesiology, SFU Burnaby, BC, Canada

ARTICLE INFO

Article history:
Accepted 18 May 2011

Keywords:
Fascicle orientation
Computational methods
Calibration

ABSTRACT

Muscle architecture is an important parameter affecting the muscle function. Most of the previous studies on *in-vivo* muscle architecture have used in 2D ultrasound. The importance of the third dimension has not been much explored due to lack of appropriate methods. DT-MRI has been used to study muscle architecture in 3D, however, due to long scan times of about 15 min DT-MRI has not been suitable to study active muscle contractions. The purpose of this study was to develop and validate methods to determine *in-vivo* muscle fascicle orientations in 3D using ultrasound. We have used 2D ultrasound and a 3D position tracker system to find the 3D fascicle orientation in 3D space. 2D orientations were obtained by using automated methods developed in our previous studies and we have extended these in the current study to obtain the 3D muscle fascicle orientation in 3D space. The methods were validated using the physical phantom and we found that the mean error in the measurement was less than 0.5° in each of the three co-ordinate planes. These methods can be achieved with short scan times (less than 2 min for the gastrocnemii) and will thus enable future studies to quantify 3D muscle architecture during sub-maximal voluntary contractions.

1. Introduction

Muscle architecture is a major determinant of the mechanical function of skeletal muscle. Muscle fascicle orientation is an important architectural parameter affecting the muscle properties. Previous studies in different species have shown regionalization of fascicle architecture in muscle and these differences in architecture have been related to differential activation patterns and function of muscles (Blazevich et al., 2006; Herring et al., 1979; Wakeling, 2009).

From the last two decades, brightness mode (B-mode) ultrasonography has been used to study muscle architecture in two dimensions (Kawakami et al., 1993; Kuno and Fukunaga, 1995). Muscle fascicle architecture can be quantified non-invasively using diagnostic ultrasound for both dynamic and isometric contractions (Fukunaga et al., 1997a; Fukunaga et al., 1997b; Ito et al., 1998; Kawakami et al., 1998; Maganaris et al., 1998). Ultrasound probes are typically less than 60 mm and so B-mode ultrasound scans do not image the whole muscle. Additionally, each scan represents a 2D slice through the muscle, and hence information in the third dimension is lost. Because of this, studies using 2D ultrasound usually image the muscle belly and implicitly assume that the 2D information from the belly is representative of the whole muscle. 3D trajectories of the muscle fascicles must be quantified in order to test the assumption that the whole muscle properties can be explained from the 2D ultrasound images of muscle belly. In order to do so, we need to develop reliable and validated methods to quantify the 3D muscle architecture across the whole muscle. Muscle fascicle structure is visible in ultrasound images for a range of probe orientations; however, the optimal alignment of the probe for 2D studies is for the muscle fascicles to lie within the scanning plane. An error of up to 23% has been reported in fascicle angles for probe orientations that do not align the fascicles with the scanning plane (Benard et al., 2009). Thus, it is also important to develop robust methods that are not sensitive to the probe orientation. Studying the muscle fascicle architecture in 3D will help to alleviate this problem.

Diffusion tensor magnetic resonance imaging (DT-MRI) has previously been used for muscle fiber tracking. The reported scan times in recent studies are at least 15 min (Budzik et al., 2007; Heemskerk et al., 2009), but active muscle contractions cannot be sustained for these durations. Also, DT-MRI is very sensitive to soft tissue motion that may occur due to prolonged contractions (Bishop et al., 2009). One notably fast DT-MRI study (2.5 min; Deux et al., 2008) reported that the diffusion co-efficient may not relate to the direction of the fascicles due to a loss of diffusion anisotropy with these rapid scans. To date, DT-MRI studies have been used mostly to study architecture in passive muscle. On the other hand, ultrasound is cheaper, and makes real-time acquisition

* Corresponding author.
E-mail addresses: mrana@sfu.ca, mankurana@gmail.com (M. Rana).

0021-9290/$ - see front matter © 2011 Elsevier Ltd. All rights reserved.
doi:10.1016/j.jbiomech.2011.05.026

possible. The faster acquisition times using ultrasound make the testing of specific experiments possible.

A few studies have used ultrasound to study 3D muscle architecture (Barber et al., 2009; Fry, 2004; Fry et al., 2003; Fry et al., 2004; Hiblar et al., 2003; Kurihara et al., 2005; Malaiya et al., 2007). 3D methods have previously studied muscle length (Fry et al., 2003; Fry et al., 2004; Malaiya et al., 2007) and volume (Barber et al., 2009) from the imaged muscle surface. 3D muscle fascicle lengths have been determined as length of a fascicle (Malaiya et al., 2007) or mean length for a few fascicles (Kurihara et al., 2005) from the belly region of the gastrocnemius muscle by manual digitization. Muscle fascicle orientation has previously been reported as the angle between a few manually digitized fascicles and either the aponeurosis (Malaiya et al., 2007) or the internal tendon of a muscle (Hiblar et al., 2003). To date, no studies have quantified a complete set of 3D fascicle orientations in the whole muscle, based on ultrasound images; this is largely due to lack of the appropriate methods.

The purpose of this study was to develop methods to study fascicle orientation in 3D across the whole muscle using B-mode ultrasound. Based on previous automated methods to determine fascicle orientation in 2D image planes (Rana et al., 2009), we have developed methods to obtain 3D fascicle orientations from 2D ultrasound and a 3D motion tracker system.

2. Methods

In order to obtain 3D muscle fascicle orientation, we collected 2D images using a linear ultrasound probe (Echoblaster, Telemed, LT) in B-mode and attached a rigid body set up made up of a cluster of three optical markers (Certus, Optotrak, NDI, Ontario), to the probe to obtain its position and orientation in 3D. We used one optotrak position sensor mounted in horizontal position to capture the rigid body markers. The motion capture system returned the position and orientation of the cluster of markers in terms of three translations and three rotations relative to the lab co-ordinate system.

The calf muscles of one male subject (height 1.83 m, weight 80 kg) were imaged using a sweeping motion of the ultrasound probe across the right leg while the subject was kneeling in a water tank. The scanning was done for passive state of muscle with knee angle maintained at 110° and ankle at 90° (Fig. 1). The leg was scanned in water immersion as this allowed the probe to be kept away from surface of skin and, hence, avoid probe pressure artifacts.

During the scanning process the probe was kept within a range of $\pm 15^{\circ}$ along the longitudinal axis of the muscle to capture the muscle fascicles from different angles (Fig. 1) and was kept 1–2 cm away from the skin surface. In order to ensure that the whole muscle was covered, a grid was drawn over the skin surface prior to scanning. The scan time depends on frame rate, speed of moving the probe and probe length. The scan time can be decreased by using a longer probe, increasing the ultrasound frame frequency or the speed of moving the probe. For a given probe, scan times can be decreased by making probe movements more rapid; however, this causes flow in the water that affects the accuracy of the ultrasound image. We used frame frequency of 20 Hz and a probe of length of 5 cm and this resulted in scan times of between 90 and 120 s to image all three muscles of the triceps surae, or a more rapid 40–60 s to image the soleus and lateral gastrocnemius.

The ultrasound images (Fig. 2A) were filtered using multiscale vessel enhancement filtering in order to enhance the line-like structures in the images and then convolved with polarized spatial wavelets to obtain local orientations in the image plane (Rana et al., 2009). 2D orientations within the image were then combined with the 3D position and orientation information from the optical system to obtain 3D fascicle orientations in lab space.

2.1. 2D orientation in each ultrasound scan

2D fascicle orientations were determined at each pixel of the ultrasound image in the image plane. The ultrasound images were filtered with the multiscale vessel enhancement filtering to suppress noise and enhance the lines representing the fascicle orientations in the image, and this was followed by the wavelet analysis on the filtered image to obtain orientations in the image plane.

For multiscale vessel enhancement, the filtered images were obtained by using methods previously described (Rana et al., 2009). A vesselness value was determined for each pixel and has a high value when the local image has a line-like structure and a low value for noisy regions with little structure (Fig. 2). For a given line-like structure, the scale value corresponding to the maximum vesselness response is related to the diameter of the line and for this study scales of 2, 3, 4 and 5 pixels were used; different image resolutions may require a different set of scales. The filtering process involved convolution with the double derivative of a Gaussian (Frangi et al., 1998), which has a wavelength $2\sqrt{3}$ times the scale value. The 2D orientation at each pixel was then obtained by convolving the filtered image with anisotropic wavelets (Rana et al., 2009). The shape of each wavelet is given by

$$G(x,y) = \exp\left(\frac{x^2+y^2}{-dk}\right)\cos\left(\frac{2\pi(x\cos\alpha - y\sin\alpha)}{\lambda}\right) + o,$$

where d is the damping of the wavelet, λ is the wavelength and o is a linear offset. The damping was set at $d=2.5622$ to (A) provide decay of the wavelet by the edges of the kernel (with a half-width of $k=19$) and (B) to satisfy the wavelet condition of zero integral (for $\alpha=0$ and $o=0$). However, due to pixilation artifacts, a non-zero value for o must be introduced for non-zero angles α in order to maintain a zero integral. For each pixel, the wavelet used for the convolution has it spatial

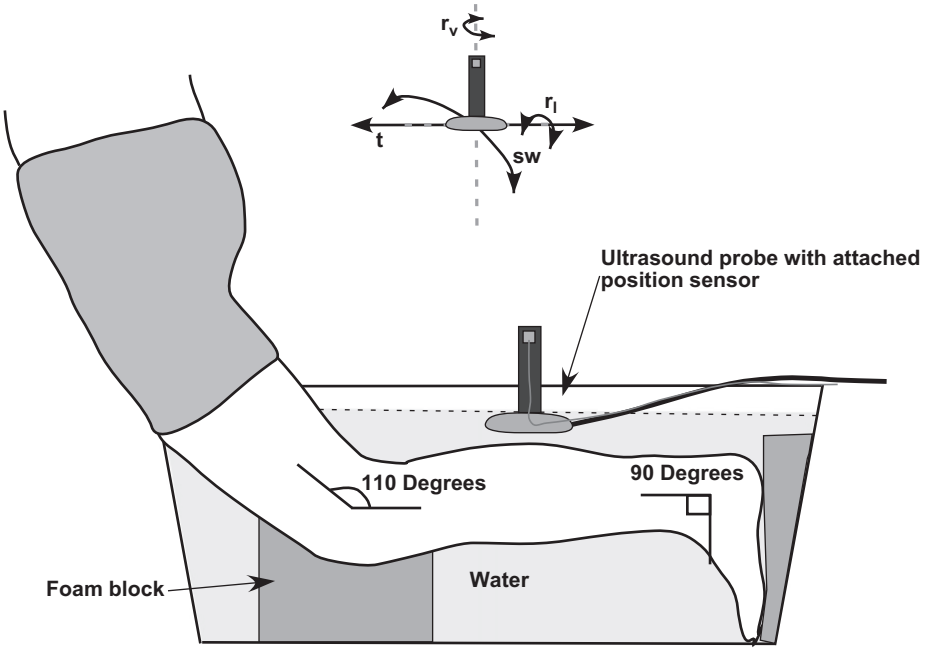

Fig. 1. Experimental setup showing the position of leg during scanning. Knee angle was maintained at 110° with the help of foam block and ankle angle at 90°. The diagram on the top represents the probe motion during scanning; translation along the muscle length (t), sweeping across the muscle width (sw), rotation along the longitudinal (r_l) and the vertical axis (r_v) of the probe.

wavelength, λ, to match the selected scale in the multiscale filtering. Four sizes of wavelets were used with λ equaling 10, 13, 16 and19.

The filtered image was convolved with a set of wavelet kernels at different orientations α. ranging from 0° to 180° with steps of 0.5°. The wavelet with orientation α that resulted in the greatest convolution for a given region in the image identified that region as having a muscle fascicle orientation of α (Rana et al., 2009).

2.2. 3D orientations of muscle fascicles

3D orientations of the muscle fascicles were determined by (A) calibrating the probe relative to the rigid body, (B) relating points in image plane (pixels) to points in 3D space (voxels), (C) transforming the orientation from 2D image plane to direction cosines in the 3D lab co-ordinate system and (D) selecting among multiple pixels from different images belonging to same voxel in space.

The ultrasound probe was calibrated with respect to the rigid body in order to determine the position of each point in the image relative to the rigid body (Dandekar et al., 2005; Prager et al., 1998). Calibration was done by scanning two parallel wires set at a constant distance z_0 from a horizontal surface (Dandekar et al., 2005). Images were taken along the cross-section of the wires and along length of the wires (Fig. 3). Two points were digitized in each image to locate the position of each of the wire in the image plane or the line formed by imaging along the length of the wires (Fig. 3). These points were transformed from the image frame of reference to the rigid body frame of reference using six unknown values (three translations and three rotations), and then from the rigid body frame to the lab co-ordinate system using the following transformations with the parameters from the optical motion capture.

$$C(x,y,z_0) = T_p^c T_i^p (su, sv, 0),$$

where $C(x,y,z_0)$ is a point in the lab co-ordinate system, (u, v) is a point in the image plane, s represents the scale between pixels and the actual distance. T_p^c is calculated using the position and orientation information of the rigid body from frame of reference relative to the lab co-ordinate system and T_i^p is the unknown transformation matrix from the image to rigid body. This can be solved for T_i^p as problem of minimization using the $z_0 = constant\ \ value$, because the points on the wires had a constant z co-ordinate in the lab co-ordinate system.

Once the calibration was known, any pixel in the image could be related to a particular voxel in lab space using the above equation. For fascicle orientations, we constructed 2D unit vectors in the image plane using the orientation values from the wavelet analysis (Rana et al., 2009) and transformed them to 3D vectors in lab space. Voxels were chosen to contain pixels from a $5 \times 5 \times 5$ mm^3 region. Due to the nature of the scanning, multiple pixels correspond to each voxel, and thus there is an over-determined series of solutions. The correct 3D fascicle orientation occurs when the fascicle lies within the image plane of the ultrasound image, and so it is defined by its 2D orientation in the image, and the orientation of that image plane. When the fascicles are in the image plane they appear as more continuous line-like structures, and this is characterized by high vesselness value from the multiscale vessel enhancement filtering, and a high convolution value from the wavelet analysis. The best solution to the 3D orientation at each voxel can thus be determined from the pixel with greatest vesselness and convolution. We have represented the 3D fascicle orientations in terms of the direction cosines of the vectors obtained.

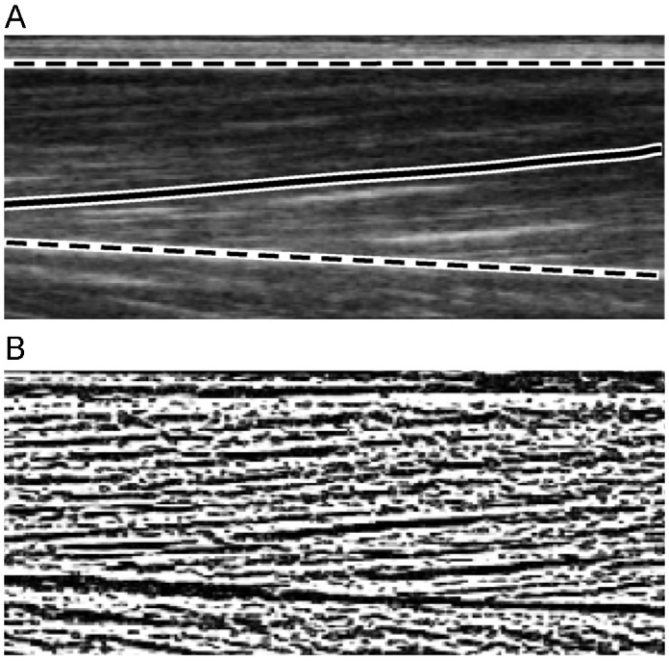

Fig. 2. Ultrasound image of lateral gastrocnemius. Aponeuroses are shown by dashed lines and muscle fascicles by bold line (A) and the image obtained after multiscale vessel enhancement filtering (B).

2.3. Validation

The methods to determine 3D muscle fascicle orientation were validated by testing them on a physical phantom (Fig. 4). The phantom was made with horse-hair stacked together in ten layers. The horse-hairs were arranged parallel to each other with the distance between adjacent hairs less than 2 mm. The hair ends were digitized using a stylus with the motion capture system to determine the orientation of hair in space. The phantom was immersed in water and scanned with a range of probe positions and orientations. Sample image from the phantom is shown in Fig. 5). The images were processed using the multiscale vessel enhancement filtering and wavelet analysis to obtain local 2D orientations of lines in the image planes. The 2D orientations were then converted to 3D direction cosines using the above methods. However, with this phantom some of the adjacent hairs partially adhered to each other and resulted in branching lines in the image. This situation is not representative of actual muscle fascicles, and resulted in the vesselness values not characterizing the orientation of the scanning plane well. Thus, in order to identify the 3D solution to the orientations and validate the methods with the phantom we just used information from the

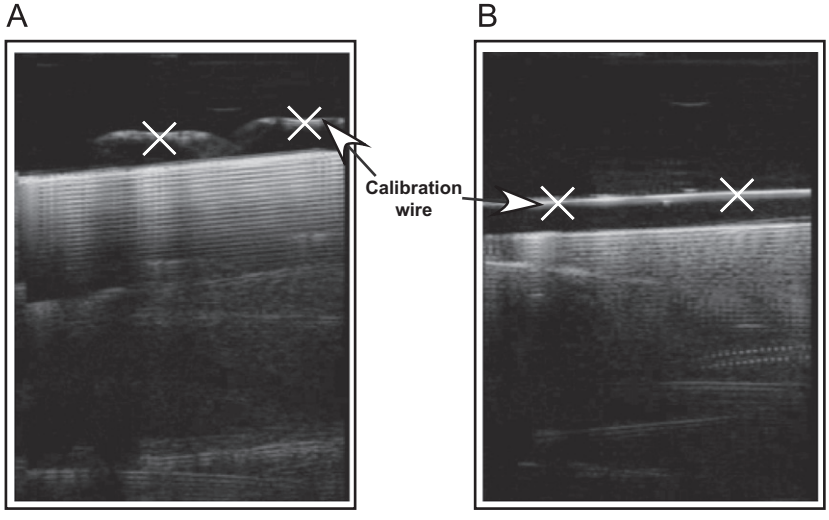

Fig. 3. Images obtained during calibration with cross sign representing the points digitized in images. Ultrasound image of the two wires imaged along the cross-section (A) and ultrasound image of a wire imaged along length of the wire (B).

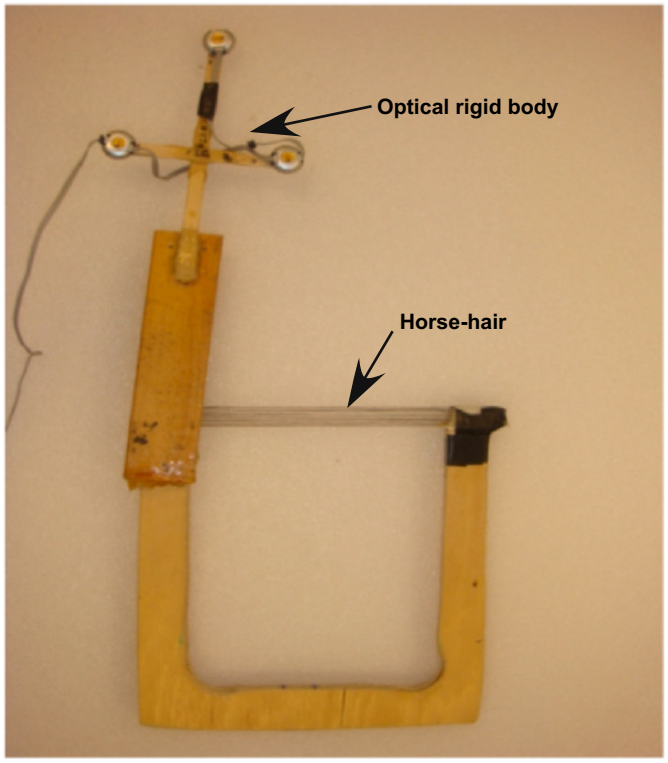

Fig. 4. Horse-hair phantom used for validation of methods. Optical rigid body was attached to track the position of the phantom while scanning.

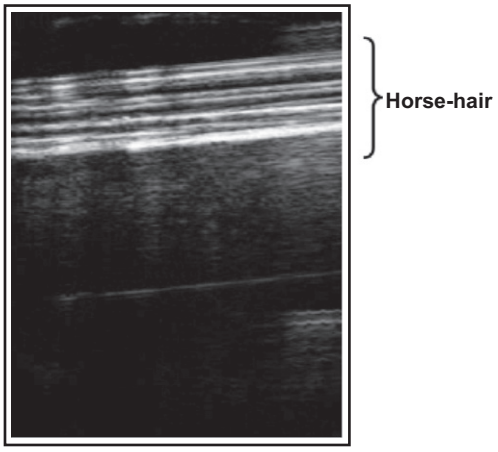

Fig. 5. Ultrasound image of horse-hair phantom used for validation.

convolution value of the wavelets to constrain the problem of multiple pixels representing each voxel.

3. Results

The methods were validated by comparing the direction cosines from digitization of the phantom to the direction cosines calculated by the above methods by finding the error of each of component of the direction cosine from the directions obtained by digitization of the hair strands. The mean errors in the *yz*, *xz* and *xy* planes are shown in Table 1. The error was calculated as the angle between the projection vectors in the three co-ordinate planes (*xy*, *yz* and *xz*) obtained from direction cosines determined by the image processing with the direction cosines from digitizing the hair stands in the phantom. The histograms for errors in the three planes spread on both sides of the zero value with peak

Table 1
Error in direction cosines in the three co-ordinate planes.

Co-ordinate plane	Mean error (deg.)	Standard deviation (deg.)
yz	−0.32	2.81
xz	−0.41	2.21
xy	0.05	2.11

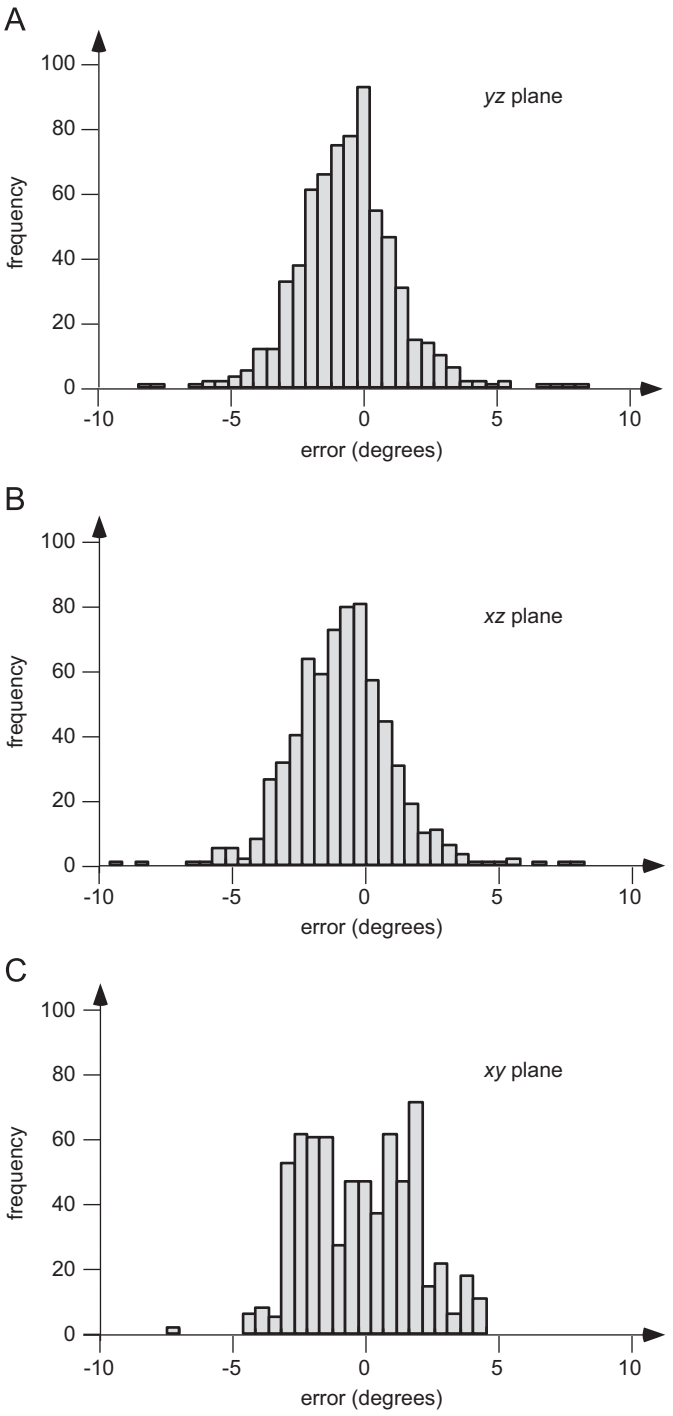

Fig. 6. Error histograms for error in estimated direction cosines in the three co-ordinate planes.

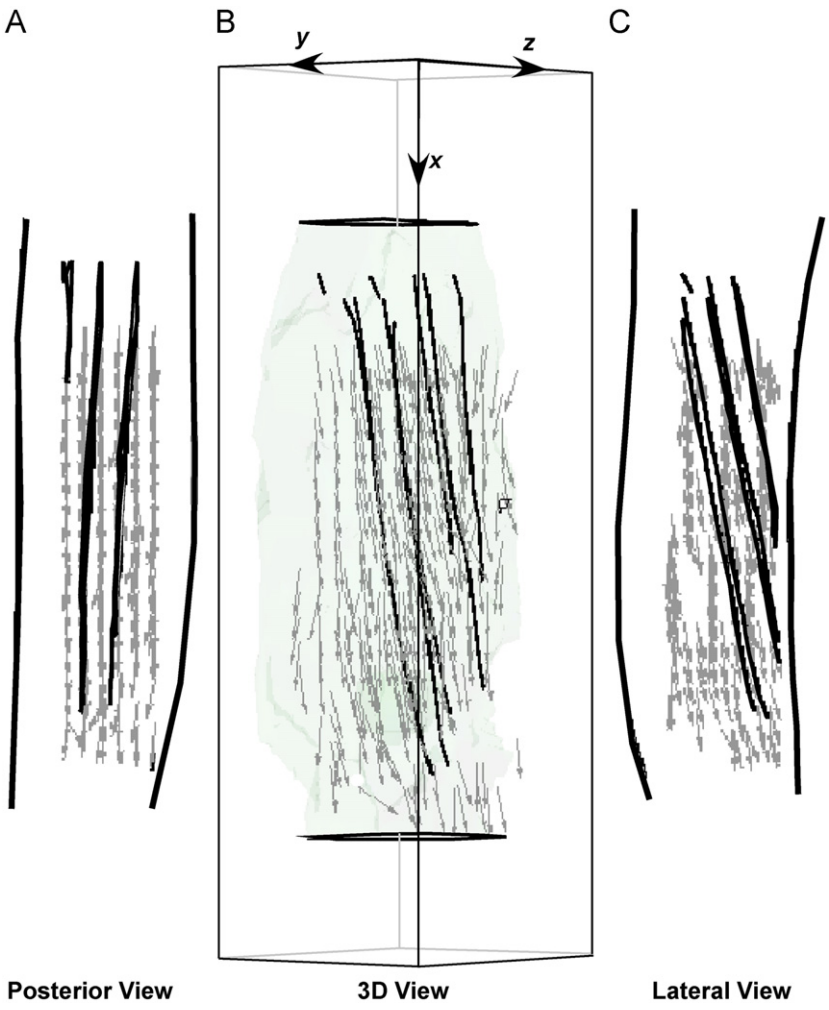

Fig. 7. Representation of 3D fascicle orientations in the lateral gastrocnemius (B). The posterior view shows the projection in *xy* plane (A) and the lateral view shows the projection in *xz* plane (C).

values close to zero for the *xz* and *yz* planes and a more distributed pattern for the vertical *xy* plane (Fig. 6).

The methods were used to obtain 3D fascicle orientations for the lateral gastrocnemius muscle. The orientations were represented as direction cosines and plotted as a vector map (Fig. 7). A few representative fascicles were tracked for visualization. Fig. 7 shows the vector grid from different views. The posterior view is along the fascicles planes and is the direction that would be typically scanned for a 2D ultrasound study; the lateral view shows the pennate nature of the fascicles.

In order to compare the results obtained from our methods with previous studies in 2D ultrasound we did the following calculations. The mean ($\pm$s.e.m.) pennation angle in the muscle belly was measured as the angle of fascicles relative to the deep aponeurosis and was $12.27 \pm 0.25^{\circ}$. The fascicle length (L_f) calculated from the pennation angle (θ) and thickness (L_t) using the following relation:

$$L_f = L_t / \sin\theta,$$

was 50.4 ± 1.8 mm.

4. Discussion

The methods described above can be used to quantify the muscle fascicle architecture in three dimensions. The methods to study the fascicle orientation in 3D were developed on the images from lateral gastrocnemius muscle and the results indicate that the methods can be used to study the *in-vivo* muscle fascicle orientation in 3D.

The mean error in predicting the orientation value is less than 0.5° in the three co-ordinate planes for the physical phantom. This error is not solely from the automated methods described above but additionally includes error due to the phantom digitization. Of note is that the hairs in the phantom bowed slightly in the vertical plane, however were assumed to lie in a straight line. Thus the actual local hair orientation varied by a couple of degrees (both positive and negative) in the *xy* plane. This effect can be seen by the more distributed range of errors in this plane (Fig. 6), and show that the methods are sufficiently sensitive to detect non-linearities in the physical phantom used for validation.

The resolution of this analysis is limited by the size of the Gauss filter for the vessel enhancement filtering and the wavelet for the wavelet analysis, and both these dictate the kernel size used for the analysis (Rana et al., 2009). The kernels were 39×39 pixels, corresponding to 5.8×5.8 mm region in the scale of ultrasound images. The voxel size selected for this analysis ($5 \times 5 \times 5$ mm) was thus close to the limit that can be resolved by this technique. Larger voxels may result in greater accuracy for angle determination, but at the cost of reduced resolution. Nevertheless, the small errors found with this technique of less than 0.5° (Table 1) mean that voxels can be kept small to combine good accuracy and resolution.

As described in the methods section, we have used the convolution value from the wavelet analysis for selecting between multiple pixels belonging to the same voxel. However, vesselness can also be used to quantify the quality of the region of image around a particular pixel. A pixel with greater vesselness value shows that the feature around that pixel relates more to a line-like structure while a smaller value indicates a disk-like or an unstructured image. Since the hairs adhered and branched on the phantom some of the lines in the image branched so were not well represented by the vesselness value. Thus, the vesselness numbers were not used to select for 3D reconstruction on the phantom but may be an important parameter to explore while studying muscle fascicle architecture.

The methods were used to calculate pennation angle and fascicle length in the belly region of the muscle. The values reported for pennation angle and fascicle length for passive muscle in previous *in-vivo* ultrasound studies are 11.3–16.7° and 41.6–74.0 mm (Chow et al., 2000; Kawakami et al., 1998; Maganaris et al., 1998; Martin et al., 2001) respectively. The measured pennation angle (12.27°) and fascicle length (50.4 mm) in this study lie within the range of previously reported values. It should be noted that fascicles may curve during contraction (Maganaris et al., 2002; Muramatsu et al., 2002; Wang et al., 2009), and the methods in this study will also allow the local fascicle orientations and thus curvature to be quantified in 3D. However, in order to compare results from these methods with previous studies, we have assumed the fascicles to be linear. The purpose of the calculations is to illustrate the application of these methods to study muscle architecture; however, further studies are needed with more subjects and more contraction conditions in order to identify how the 3D muscle fascicle orientations change during contraction.

Most of the previous studies on determination of muscle fascicle length or orientation have involved manual selection of fascicles in 3D muscle image to find fascicle length (Kurihara et al., 2005; Malaiya et al., 2007) and angle of fascicles relative to internal tendon (Hiblar et al., 2003). Manual digitization can be subjective and time consuming for studying the whole muscle architecture. All the processing for determination of 3D fascicle orientation in our methods is automated. This makes it possible to study architecture in whole muscle and also to compare the orientation changes in muscle with different contraction levels.

Our testing protocol has reduced some of the difficulties to studying 3D architecture *in-vivo*. Data collection in water allows the sweeping motion of probe but may prohibit studies that involve simultaneous electrical stimulation or EMG collection. The short scan times of less than two minutes will enable submaximal contractions to be studied, but are still too long to study non-isometric contractions or maximum voluntary contraction. We have used these methods to quantify the 3D architecture in triceps surae muscle for different force levels and ankle angles, and these data will be reported elsewhere. Since the fascicle orientations are initially determined in 2D and then converted to 3D, these methods can be only be used to study the 3D architecture in muscles whose fascicle structure is visible in 2D ultrasound scans.

Our methods can be used to determine *in-vivo* muscle fascicle orientation in 3D. The methods provide a tool to quantify the regionalization of fascicle orientation in the muscle and study the changes in 3D fascicle architecture in isometrically contracting muscle. Having reliable methods to quantify the architecture in 3D will enable future studies to test the importance of the third dimension in the relation between muscle architecture and function.

Conflict of interest statement

There is no conflict of interest.

Acknowledgments

We thank Dr. Robert N. Rohling for helpful discussion on calibration of the ultrasound probe and thank NSERC for financial support to J.W.

References

Barber, L., Barrett, R., Lichtwark, G., 2009. Validation of a freehand 3D ultrasound system for morphological measures of the medial gastrocnemius muscle. J. Biomech. 42 (9), 1313–1319.

Benard, M.R., Becher, J.G., Harlaar, J., Huijing, P.A., Jaspers, R.T., 2009. Anatomical information is needed in ultrasound imaging of muscle to avoid potentially substantial errors in measurement of muscle geometry. Muscle Nerve 39 (5), 652–665.

Bishop, M.J., Hales, P., Plank, G., Gavaghan, D.J., Scheider, J., Grau, V., 2009. Comparison of Rule-Based and DTMRI-Derived Fibre Architecture in a Whole Rat Ventricular Computational Model. Springer, Berlin/Heidelberg.

Blazevich, A.J., Gill, N.D., Zhou, S., 2006. Intra- and intermuscular variation in human quadriceps femoris architecture assessed in vivo. J. Anat. 209 (3), 289–310.

Budzik, J.F., Le Thuc, V., Demondion, X., Morel, M., Chechin, D., Cotten, A., 2007. In vivo MR tractography of thigh muscles using diffusion imaging: initial results. Eur. Radiol. 17 (12), 3079–3085.

Chow, R.S., Medri, M.K., Martin, D.C., Leekam, R.N., Agur, A.M., McKee, N.H., 2000. Sonographic studies of human soleus and gastrocnemius muscle architecture: gender variability. Eur. J. Appl. Physiol. 82 (3), 236–244.

Dandekar, S., Li, Y., Molloy, J., Hossack, J., 2005. A phantom with reduced complexity for spatial 3-D ultrasound calibration. Ultrasound Med. Biol. 31 (8), 1083–1093.

Deux, J.F., Malzy, P., Paragios, N., Bassez, G., Luciani, A., Zerbib, P., Roudot-Thoraval, F., Vignaud, A., Kobeiter, H., Rahmouni, A., 2008. Assessment of calf muscle contraction by diffusion tensor imaging. Eur. Radiol. 18 (10), 2303–2310.

Frangi, A.F., Niessen, W.J., Vincken, K.L., Viergever, M.A., 1998. Multiscale vessel enhancement filtering. MICCAI 1496, 130–137.

Fry, A.C., 2004. The role of resistance exercise intensity on muscle fibre adaptations. Sports Med. 34 (10), 663–679.

Fry, N.R., Childs, C.R., Eve, L.C., Gough, M., Robinson, R.O., Shortland, A.P., 2003. Accurate measurement of muscle belly length in the motion analysis laboratory: potential for the assessment of contracture. Gait Posture 17 (2), 119–124.

Fry, N.R., Gough, M., Shortland, A.P., 2004. Three-dimensional realisation of muscle morphology and architecture using ultrasound. Gait Posture 20 (2), 177–182.

Fukunaga, T., Ichinose, Y., Ito, M., Kawakami, Y., Fukashiro, S., 1997a. Determination of fascicle length and pennation in a contracting human muscle in vivo. J. Appl. Physiol. 82 (1), 354–358.

Fukunaga, T., Kawakami, Y., Kuno, S., Funato, K., Fukashiro, S., 1997b. Muscle architecture and function in humans. J. Biomech. 30 (5), 457–463.

Heemskerk, A.M., Sinha, T.K., Wilson, K.J., Ding, Z., Damon, B.M., 2009. Quantitative assessment of DTI-based muscle fiber tracking and optimal tracking parameters. Magn. Reson. Med. 61 (2), 467–472.

Herring, S.W., Grimm, A.F., Grimm, B.R., 1979. Functional heterogeneity in a multipinnate muscle. Am. J. Anat. 154 (4), 563–576.

Hiblar, T., Bolson, E.L., Hubka, M., Sheehan, F.H., Kushmerick, M.J., 2003. Three dimensional ultrasound analysis of fascicle orientation in human tibialis anterior muscle enables analysis of macroscopic torque at the cellular level. Adv. Exp. Med. Biol. 538, 635–644 (discussion 645).

Ito, M., Kawakami, Y., Ichinose, Y., Fukashiro, S., Fukunaga, T., 1998. Nonisometric behavior of fascicles during isometric contractions of a human muscle. J. Appl. Physiol. 85 (4), 1230–1235.

Kawakami, Y., Abe, T., Fukunaga, T., 1993. Muscle-fiber pennation angles are greater in hypertrophied than in normal muscles. J. Appl. Physiol. 74 (6), 2740–2744.

Kawakami, Y., Ichinose, Y., Fukunaga, T., 1998. Architectural and functional features of human triceps surae muscles during contraction. J. Appl. Physiol. 85 (2), 398–404.

Kuno, S., Fukunaga, T., 1995. Measurement of muscle fibre displacement during contraction by real-time ultrasonography in humans. Eur. J. Appl. Physiol. Occup. Physiol. 70 (1), 45–48.

Kurihara, T., Oda, T., Chino, K., Kanehisa, H., Fukunaga, T., Kawakami, Y., 2005. Use of three-dimensional ultrasonography for the analysis of the fascicle length of human gastrocnemius muscle during contractions. Int. J. Sport Health Sci. 3, 226–234.

Maganaris, C.N., Baltzopoulos, V., Sargeant, A.J., 1998. In vivo measurements of the triceps surae complex architecture in man: implications for muscle function. J. Physiol. 512 (Pt. 2), 603–614.

Maganaris, C.N., Baltzopoulos, V., Sargeant, A.J., 2002. Repeated contractions alter the geometry of human skeletal muscle. J. Appl. Physiol. 93 (6), 2089–2094.

Malaiya, R., McNee, A.E., Fry, N.R., Eve, L.C., Gough, M., Shortland, A.P., 2007. The morphology of the medial gastrocnemius in typically developing children and children with spastic hemiplegic cerebral palsy. J. Electromyogr. Kinesiol. 17 (6), 657–663.

Martin, D.C., Medri, M.K., Chow, R.S., Oxorn, V., Leekam, R.N., Agur, A.M., McKee, N.H., 2001. Comparing human skeletal muscle architectural parameters of cadavers with in vivo ultrasonographic measurements. J. Anat. 199 (Pt. 4), 429–434.

Muramatsu, T., Muraoka, T., Kawakami, Y., Shibayama, A., Fukunaga, T., 2002. In vivo determination of fascicle curvature in contracting human skeletal muscles. J. Appl. Physiol. 92 (1), 129–134.

Prager, R.W., Rohling, R.N., Gee, A.H., Berman, L., 1998. Rapid calibration for 3-D freehand ultrasound. Ultrasound Med. Biol. 24 (6), 855–869.

Rana, M., Hamarneh, G., Wakeling, J.M., 2009. Automated tracking of muscle fascicle orientation in B-mode ultrasound images. J. Biomech. 42 (13), 2068–2073.

Wakeling, J.M., 2009. The recruitment of different compartments within a muscle depends on the mechanics of the movement. Biol. Lett. 5 (1), 30–34.

Wang, H.K., Wu, Y.K., Lin, K.H., Shiang, T.Y., 2009. Noninvasive analysis of fascicle curvature and mechanical hardness in calf muscle during contraction and relaxation. Man. Ther. 14 (3), 264–269.